

Investigation of the anisotropic deuterium ordering in α -LuD single crystals by resistivity and heat-capacity measurements

P. Vajda, J. N. Daou, and J. P. Burger

Hydrogène et Défauts dans les Métaux, Bâtiment 350, Université de Paris—Sud, F-91405 Orsay, France

K. Kai,* K. A. Gschneidner, Jr., and B. J. Beaudry

Ames Laboratory and Department of Materials Science and Engineering, Iowa State University, Ames, Iowa 50011

(Received 21 April 1986)

The electrical resistivity and the heat capacity of single crystals of LuD_{0.183} were measured from ~ 1 to 300 K. An anomaly due to ordering of deuterium pairs along the *c* axis is observed in both the resistivity and heat-capacity measurements. The binding energy of the ordered state is $\sim 15\%$ larger in the *c* direction than in the *a* direction. Rapid cooling of the samples across the anomaly quenched in the single D atoms of the room-temperature α solid-solution phase giving rise to a resistivity increase $\Delta\rho_q$, which recovers in the anomaly region upon heating. No anisotropic effect was observed in $\Delta\rho_q$ as expected. The heat-capacity data show a small thermal effect at ~ 200 K and an unusual flattening of the C_p versus T curve between 70 and 190 K. This flattening is thought to be due to a stiffening of the lattice, which seems to peak at the anomaly temperature.

I. INTRODUCTION

Lutetium—like several other hcp rare earths—forms with hydrogen a solid solution, α -LuH_{*x*}, which is stable down to 4.2 K for $x \leq 0.20$ at. H/at. Lu.¹ This system exhibits an anomaly with an *x*-dependent amplitude in the electrical resistivity at 160–170 K, which manifests an isotope effect (higher anomaly temperature for α -LuD_{*x*}), and which has been investigated in detail by the group at Orsay. It has been shown that a quench across the anomaly temperature introduced defects resulting in an increase of the residual resistivity, $\Delta\rho$, in the same way as low-temperature electron irradiation leads to an increase. In both cases the defects recover in the anomaly region.^{2,3} Further experiments concerned the observation of a hydrogen Snoek effect in low-frequency internal friction on α -LuH(D)_{*x*};⁴ the localization of deuterium atoms in tetrahedral (*T*) interstitial sites of the lutetium lattice through ion beam channeling in α -LuD_{*x*} crystals;⁵ and the determination of static and dynamic displacements around H atoms in α -LuH_{*x*} crystals by energy-dispersive x-ray diffraction.⁶ The anomaly was attributed to short-range ordering of hydrogen into H-H pairs along the *c* axis,⁷ the detailed structure being determined recently in neutron-scattering experiments⁸ as linear ordering of second-neighbor pairs along *c*, with a Lu atom in between. In view of the manifest anisotropy of the hydrogen ordering at low temperatures, it was therefore interesting to investigate the resistivity anomaly on single-crystal specimens in different directions. In what follows, we are presenting results obtained with single crystals of α -LuD_{0.183} oriented along the *a* axis and the *c* axis. In addition low-temperature (1–300 K) heat-capacity measurements were made on the LuD_{0.183} sample from which the single-crystal resistivity samples had been cut, in order to determine the nature and magnitude of the thermal effects.

II. EXPERIMENTAL PROCEDURES

A. Sample preparation

The Lu metal was prepared by the Materials Preparation Center of the Ames Laboratory by the standard metallothermic reduction of the fluoride followed by distillation.⁹ A chemical analysis of the Lu metal is given in Table I. A single crystal was prepared by arc melting 172 g of Lu and annealing it at 1500°C for 40 h. A bicrystal resulted and was cut into two single crystals weighing 70 and 100 g each. The smaller crystal was electropolished and deuterium was added according to the following procedure. After placing the crystal in the deuteriding system, it was evacuated to 2×10^{-7} torr, and the sample was heated slowly until a temperature of 650°C was attained. With the Lu crystal isolated, a known volume was filled with deuterium to the desired pressure necessary to give a ~ 15 at. % D-Lu alloy. To keep the surface damage of the crystal to a minimum, the deuterium was admitted to the chamber containing the Lu sample in five equal increments. In each increment all of the deuterium was absorbed within one minute. The temperature of 640°C was maintained for at least 8 h between additions of deuterium to allow the LuD₂ which formed on the surface to diffuse

TABLE I. Chemical analysis of lutetium listing only impurities present at a level of 10 ppm atomic or more.

Impurity	Concentration	Impurity	Concentration
H	865	Fe	24
C	336	Ni	16
N	112	Cu	10
O	1635	Gd	12
F	<27		

into the sample. After the final increment of deuterium had been added the single crystal was held at 640°C for an additional 600 h to ensure equilibrium.

Four samples were cut from four different locations for vacuum fusion analysis. The results of the analysis gave a composition of $\text{LuD}_{0.183 \pm 0.003}$ indicating that the deuterium concentration was uniform throughout the sample. Metallographic examination of a section showed that no second phase was present. The crystal was oriented and cut into several different shapes. The largest one was used for the heat-capacity measurements. Four samples were cut to the approximate dimensions of $1 \times 1 \times 10$ mm (two had an *a* axis parallel to the long dimension and two had a *c* axis parallel to the long dimension) for resistivity studies.

B. Resistivity measurements

The actual sample dimensions for resistivity measurements were as follows: with the *c* axis parallel to the long dimension, $13 \times 0.78 \times 1.30$ mm; with the *a* axis parallel to the long dimension, $13 \times 0.96 \times 1.10$ mm. Platinum lead wires were spot welded onto the ends of the samples, and the resistances were measured by using the standard dc four-point method. The measurements were taken with increasing temperature. The absolute precision was several percent, because of the uncertainties in determin-

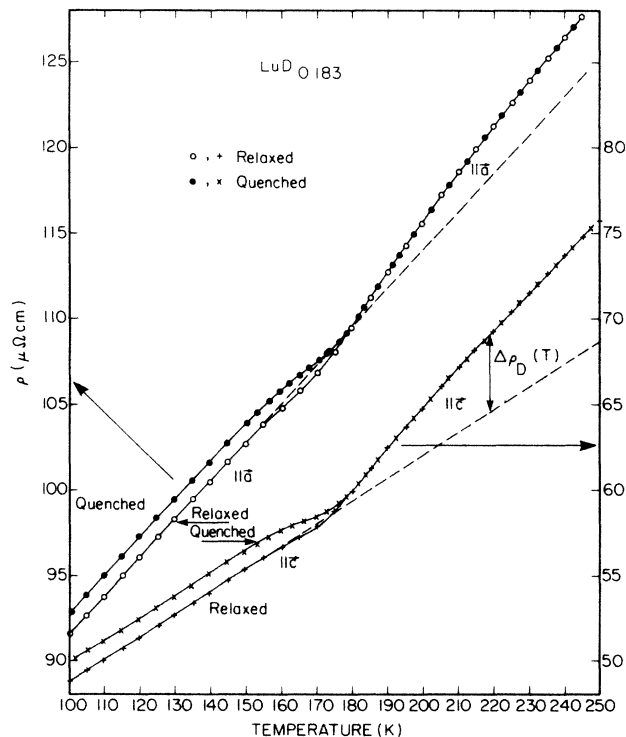


FIG. 1. Temperature dependence of the resistivities of relaxed and quenched $\alpha\text{-LuD}_{0.183}$ crystals parallel to the *c* axis and the *a* axis. The straight lines are the linearly extrapolated $\rho(T)$ dependences of the low-temperature behavior into the region above the anomaly, indicating the contribution of deuterium disorder, $\Delta\rho_D(T)$.

ing the shape factor; the relative precision on the same sample when varying the temperature was $\sim 10^{-8}$ Ω cm on a (ρ, T) couple. The temperature was measured with a calibrated platinum resistor. The cooling of the samples to liquid helium occurred either in a slow regime, ~ 0.5 K/min (relaxed specimens), or at a cooling rate of an order of magnitude faster, ~ 5 K/min, to yield quenched specimens. The residual resistivities of the $\text{LuD}_{0.183}$ crystals were

$$\rho_a(4.2 \text{ K}) = 71.5 \mu\Omega \text{ cm}$$

and

$$\rho_c(4.2 \text{ K}) = 40.2 \mu\Omega \text{ cm}.$$

The residual resistivity ratios (RRR) $\mathcal{R} \equiv R_{293 \text{ K}}/R_{4.2 \text{ K}}$ were $\mathcal{R}_a = 1.94$ and $\mathcal{R}_c = 2.11$.

C. Calorimetry measurements

Two low-temperature calorimeters were used in this study and are of the usual isolation heat-pulse type with a mechanical heat switch. One calorimeter was used for making measurements from 1.4 to 20 K (Ref. 10) and the other was used over the range from 20 to 300 K.¹¹ A 13.88 g sample was cut from the 70 g single crystal for the heat-capacity measurements. The $\text{LuD}_{0.183}$ was slowly cooled down to either 4.2 or 20 K depending upon the calorimeter and should be considered to be in the relaxed state.

III. RESULTS AND DISCUSSION

A. Resistivity

1. Presentation of the anomaly

Shown in Fig. 1 is the temperature dependence of the resistivities in the *a* and *c* directions, both in the relaxed state (after slow cooling) and after a quench across the anomaly. We shall first discuss the relaxed specimens.

As a general observation, the basal-plane specimens have higher resistivities than the *c*-axis specimens, by 40 to 50 $\mu\Omega$ cm in the region between 100 and 200 K, in conformity with the pure metal (Boys and Legvold¹² had measured 20 to 30 $\mu\Omega$ cm more for a *b*-oriented crystal than for a *c* crystal of pure Lu in the same temperature range). A comparison with the resistivity of polycrystalline $\alpha\text{-LuD}_{0.18}$ (Ref. 3) shows that the polycrystalline resistivity lies between the values for the *a* and *c* crystals of $\alpha\text{-LuD}_{0.183}$.

The striking observation concerning the manifestation of the anomaly is that the break around 170–180 K is much stronger in the case of the *c* crystal than for the *a* crystal, a fact underlined by the straight-line extrapolation of the low-temperature resistivity into the region above the anomaly. The slopes which are nearly twice as large for the *a* sample below the anomaly become comparable to one another above 210 K,

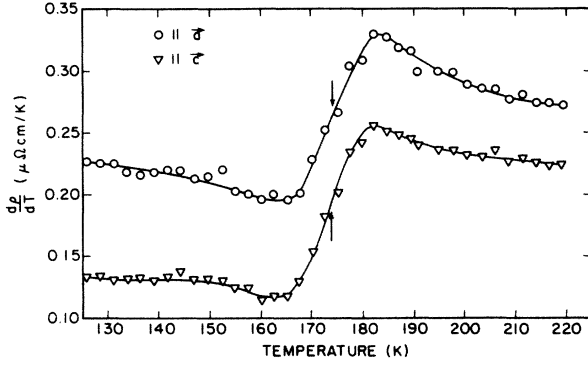


FIG. 2. Temperature derivatives, $d\rho/dT$, for the relaxed crystals of Fig. 1 indicating the anomaly temperatures.

$$\left. \begin{aligned} \frac{d\rho_a}{dT} &= 0.20 \text{ to } 0.22 \mu\Omega \text{ cm/K} \\ \frac{d\rho_c}{dT} &= 0.12 \text{ to } 0.13 \mu\Omega \text{ cm/K} \end{aligned} \right\} \text{ for } T \leq 160 \text{ K ,}$$

$$\left. \begin{aligned} \frac{d\rho_a}{dT} &= 0.25 \text{ to } 0.26 \mu\Omega \text{ cm/K} \\ \frac{d\rho_c}{dT} &= 0.22 \text{ to } 0.23 \mu\Omega \text{ cm/K} \end{aligned} \right\} \text{ for } T \geq 210 \text{ K .}$$

It is interesting to note that the slopes in the case of the pure metal were different by a factor of 2 at high temperatures:¹² $d\rho_b/dT = 0.25 \mu\Omega \text{ cm/K}$, $d\rho_c/dT = 0.12 \mu\Omega \text{ cm/K}$ which are close to our low-temperature slopes. The polycrystalline samples of Ref. 3 exhibited intermediate slopes between the anomaly: $d\rho/dT = 0.17$ to $0.18 \mu\Omega \text{ cm/K}$ for $T \leq 160 \text{ K}$ and roughly the same as the single crystals above the anomaly.

Figure 2 shows a detailed view of the anomaly area through a differentiated representation. This permits a precise determination of the anomaly temperature, which is defined as the center of the change-of-slope region,

$$T_{\text{an}} = 174 \pm 0.5 \text{ K ,}$$

which is independent of orientation within the precision of our measurement. We recall that, for the polycrystalline $\text{LuD}_{0.18}$ sample³ $T_{\text{an}} = 172 \pm 1 \text{ K}$ which is in fair agreement with the present data.

2. Binding energies

One can calculate the binding energy of the ordered low-temperature structure, as had been done earlier for the polycrystals,³ by supposing a thermally activated process for its destruction. Then, the difference $\Delta\rho_D$ between the measured temperature dependence of the resistivity in the region above the anomaly and the $\rho(T)$ extrapolated from below it can be fitted by a Boltzmann form such that

$$\Delta\rho_D(T) \propto \exp(-E_b/k_B T) . \quad (1)$$

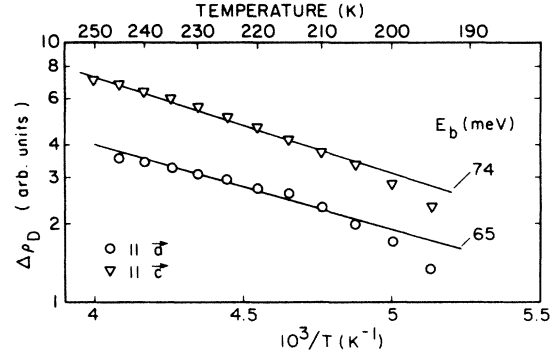


FIG. 3. Arrhenius plots of the $\Delta\rho_D$ from Fig. 1 for the calculation of the binding energies of the ordered state.

After determining this difference (see Fig. 1) one obtains the binding energies as the slopes of the straight lines in an Arrhenius plot (Fig. 3),

$$E_b^{\parallel a}(D) = 65 \pm 3 \text{ meV ,}$$

and

$$E_b^{\parallel c}(D) = 74 \pm 3 \text{ meV .}$$

These values are close to the binding energies determined for polycrystalline samples,³ $E_b^{\text{poly}}(D) = 73 \pm 5 \text{ meV}$. The interesting observation is, however, the clear orientational dependence of E_b ,

$$E_b^{\parallel c}/E_b^{\parallel a} = 1.14 \pm 0.06 .$$

3. Quenched samples

We have also undertaken a quenching experiment by rapidly cooling the specimens across the anomaly. The introduced $\Delta\rho_q$ superposes upon the residual resistivity and is shown in Fig. 1. We have investigated the annealing behavior of $\Delta\rho_q$ for both crystals by comparing the $\rho(T)$ before and after quench, and have plotted this difference in Fig. 4. One notes practically identical behavior for the a and c crystals: They recover in one smooth annealing stage right in the anomaly region which is presented in a differentiated form in the inset of Fig. 4. The peak temperature T_p for this stage is

$$T_p = 171 \text{ K .}$$

One can analyze the annealing behavior by assuming a single activated process at its origin with a constant activation energy, E_m , for migration of the recovering defect. Then, the rate of change in the concentration, n , of the annealing species, can be treated by a chemical rate equation of the form,¹³

$$\frac{dn}{dt} \propto n^\gamma \exp(-E_m/k_B T) , \quad (2)$$

where γ is the reaction order. It was shown in previous work³ that $\gamma = 1$, i.e., the reaction was of first order—either diffusion to a fixed number of sinks or a kind of close-pair recombination. Then, supposing a proportionality between $\Delta\rho$ and n , and working in a constant

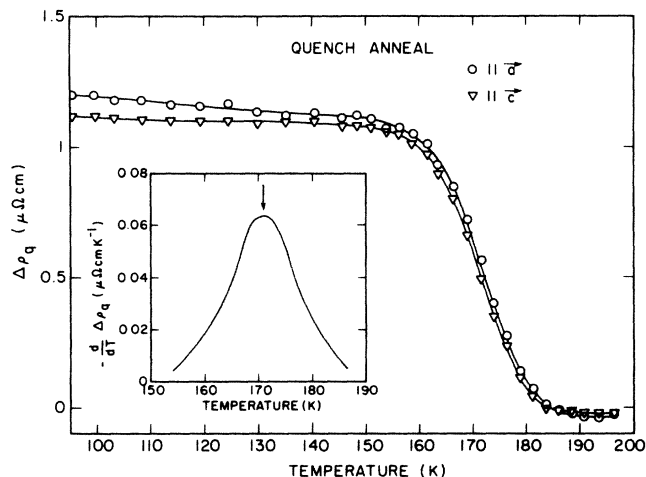


FIG. 4. Annealing behavior of the quenched-in $\Delta\rho_q(T) \equiv \rho_q(T) - \rho_{rel}(T)$ for both α - $\text{LuD}_{0.183}$ crystals. The inset shows the derived recovery peak in the case of the c crystal (the derived recovery peak for the a crystal is practically indistinguishable from the c -axis behavior).

heating-rate regime, $\Delta T \propto \Delta t$, one can determine the migration energy from Eq. (2),

$$E_m = k_B T_p^2 \frac{d\Delta\rho(T_p)}{dT} [\Delta\rho(T_p)]^{-1} \quad (3)$$

by measuring the value of $\Delta\rho(T_p)$ and its derivative at the peak temperature. One obtains then

$$E_m = (0.25 \text{ to } 0.30) \text{ eV},$$

the same, within the measuring precision, for both crystal orientations. For the polycrystalline³ samples $E_m = (0.26 \pm 0.02) \text{ eV}$ which is in accord with the single-crystal results.

4. Other comments

The above described findings of the resistivity measurements on single crystals of α - $\text{LuD}_{0.183}$ can be readily discussed and understood within the framework of the linear short-range ordered structure as established by neutron scattering.⁸ In this structure (see Fig. 5), the deuterium atoms order in pairs along the c axis, occupying second-neighbor T sites distant $\frac{3}{4}c$ from each other. Moreover, they form short chains where the links (D-D pairs) are shifted by $a/\sqrt{3}$ along the b axis. This explains at once the anisotropy in the binding energy determined for our single crystals: $E_b^{||c} > E_b^{||a}$. Supposing E_b to consist of two contributions—an “intramolecular” between the D atoms of a pair and an “intermolecular” between two D-D links in the chain—one can consider the former to be isotropic. Then, in the anisotropic part, the smaller $E_b^{||a}$ reflects the correlation between chain links in the basal plane.

Another interesting point is that the strong anisotropy of the slopes $d\rho/dT$ below the anomaly has nearly disappeared above it (Fig. 2). Now, as has been discussed by Legvold,¹⁴ the ratio of the slopes in the c direction and

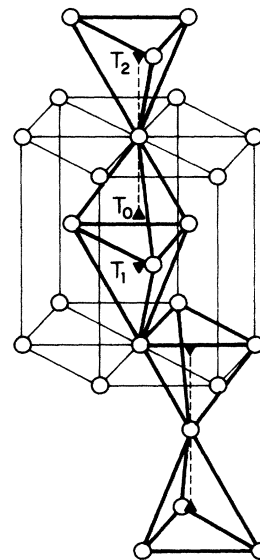


FIG. 5. Hexagonal close-packed unit cell of LuD_x showing the various tetrahedral sites. T_0T_1 and T_0T_2 are the nearest and the second-neighbor sites along the c axis. The dashed lines indicate two D-D pairs aligned in a quasilinear configuration as determined through neutron scattering (Ref. 8).

perpendicular to it is inverse to the ratio between the Fermi-surface projections upon these directions,

$$\frac{d\rho_a/dT}{d\rho_c/dT} = \frac{\int_{E_F} dS_c}{\int_{E_F} dS_a}. \quad (4)$$

Thus, the Fermi-surface anisotropy in Lu metal, expressed by the ratio

$$\frac{d\rho_b/dT}{d\rho_c/dT} = 2.1$$

calculated by Legvold from Ref. 12, has been efficiently suppressed by randomly dissolved deuterium atoms, as concluded from the high-temperature ratio

$$\frac{d\rho_a/dT}{d\rho_c/dT} \approx 1.1.$$

In the low-temperature ordered state, however, the linear D-D chains in the c direction reactivate the Fermi-surface anisotropy leading to a slope ratio

$$\frac{d\rho_a/dT}{d\rho_c/dT} = 1.7 \text{ to } 1.8.$$

Finally, the quench does not seem to yield anisotropy effects. This is not surprising, since its introduced $\Delta\rho_q$ represents the contribution of frozen-in statistically distributed single D atoms of the high-temperature α phase, with no orientational preference. In the same way, there is no difference with respect to their activation energies, in view of the three-dimensional migration mechanism for diffusion.

B. Heat capacity

The low-temperature heat capacity of $\text{LuD}_{0.183}$ is shown in Fig. 6. The data below 7 K were used to extract the electronic specific heat constant, γ , and the Debye temperature Θ_D by the standard technique (a least-squares fit of the data to C/T versus T^2 plot). The resultant values, $\gamma = 6.73$ mJ/g-at. K^2 and $\Theta_D = 200$ K, compare quite well with the values reported by Thome *et al.*¹⁵ for $\text{LuH}_{0.181}$ ($\gamma = 6.964$ mJ/g-at. K^2 and $\Theta_D = 204.9$ K). Two anomalies are evident in the heat-capacity curve—a small peak centered at 203 K and an unusual flattening of the heat capacity from ~ 70 to ~ 190 K.

The small peak is thought to be due to the ordering of the D atoms into D-D pairs, which takes place upon cooling from 223 to 183 K, a span on 40 K. The entropy associated with this ordering is 0.09 eu, but since there is 15.44% D in this alloy, the entropy per D atom is 0.58. This value compares favorably with the total entropy for the four-ordering processes observed in LaD_3 —0.56 eu/D atom.¹¹

The difference in the anomaly temperature (174 K) found in the resistivity measurements and the peak in the heat-capacity data (183 to 223, with a mean of 203 K) may seem difficult to explain. The thermal data suggest that formation of D pairs along the c axis starts to occur at ~ 220 K upon cooling and that the ordering is complete at ~ 180 K just above the temperature at which the resistivity anomaly is most apparent. A close examination of Fig. 1 shows that the straight line established at high temperatures begins to deviate at ~ 215 K in accord with the thermal data. It appears that the ordering of D pairs is most manifested in the resistivity just as the final atoms are ordered. We also wish to point out in this context that the deuterium-relaxation peak of $\alpha\text{-LuD}_x$ in the low-frequency internal friction experiments⁴ also occurred

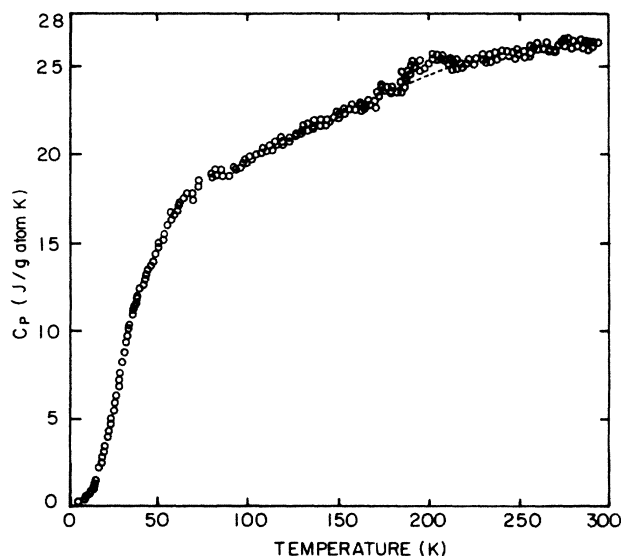


FIG. 6. Heat capacity of $\text{LuD}_{0.183}$ from 1.2 to 300 K. To obtain the heat capacity of $\text{LuD}_{0.183}$ in units of J/mole K multiply the values listed by 1.183.

slightly above 200 K indicating the region of the start of the ordering.

In order to understand the flattening of the C versus T curve, one might be tempted to compare the heat-capacity curves of $\text{LuD}_{0.183}$ (i.e., 15.44 at. % D) and pure lutetium. But since the electronic and lattice contributions to the heat capacities are significantly different (i.e., the γ values differ by $\sim 22\%$ and the Θ_D values by $\sim 9\%$), this procedure is not too meaningful. To eliminate the differences in the electronic contributions (C_E) we subtracted the respective γT values from the measured heat capacities, and the resultant values are called the "lattice" contributions (C_L). The C_L versus temperature curve for $\text{LuD}_{0.183}$ is plotted as the solid line in Fig. 7 and is labeled as $C_L(\text{obs})$. In order to estimate the expected lattice contribution for $\text{LuD}_{0.183}$ [$C_L(\text{calc})$] we have assumed that the temperature dependence of Θ_D of $\text{LuD}_{0.183}$ is the same as that of pure Lu. The Debye temperature of Lu at $T > 0$ K was calculated from $C_L(\text{obs})$ of Lu from the following relationship:¹⁶

$$C_L = 9R \left(\frac{T}{\Theta_D} \right)^3 \int_0^{x_D} \frac{x^4 e^x}{(e^x - 1)^2} dx, \quad (5)$$

where $x_D = \Theta_D/T$ and R is the gas constant, using the tables of Kilpatrick and Sherman.¹⁷ The data of Thome *et al.*¹⁵ from 1.1 to 19.1 K and that of Jennings *et al.*¹⁸ from 15 to 350 K for Lu were used to construct the $\Theta_D(T)/\Theta_D(0)$ versus T plot. This plot was then used to estimate $\Theta_D(T)$ for $\text{LuD}_{0.183}$ which in turn by using the above relation [Eq. (5)] yielded $C_L(\text{calc})$, which is plotted as the dashed curve in Fig. 7.

It is seen that $C_L(\text{obs})$ and $C_L(\text{calc})$ are in good agreement below 60 K and above 240 K, and that the flattening of the experimental data is quite obvious, when compared to the normal lattice heat capacity shown by the dashed curve. This flattening could be accounted for by a stiffening of the lattice due to ordering of the D atoms as described earlier. This stiffening which leads to a lower heat capacity should also be evident in the temperature dependence of the Debye temperature. A plot of Θ_D

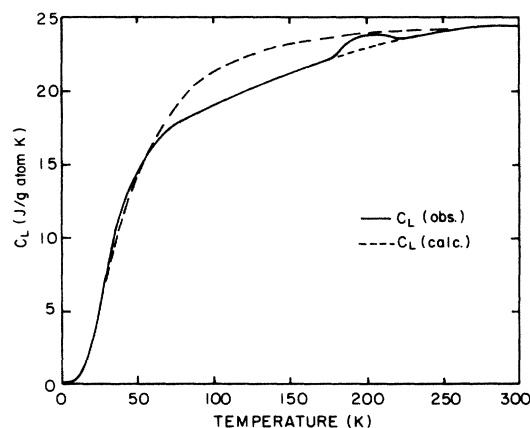


FIG. 7. Lattice contribution to the heat capacity of $\text{LuD}_{0.183}$ from 1.2 to 300 K. To obtain the heat capacity of $\text{LuD}_{0.183}$ in units of J/mole K multiply the values listed by 1.183.

versus temperature for $\text{LuD}_{0.183}$ using the same procedure as described above for Lu is shown in Fig. 8. For comparison purposes the temperature dependence of the Θ_D of a normal material (Lu) is also shown. It should be noted that the scale for Lu has been shifted upward and that its $\Theta_D(0)$ value is 17 K lower than that of $\text{LuD}_{0.183}$. The large increase in Θ_D for $\text{LuD}_{0.183}$ especially in the range 70 to 220 K is obvious when compared to the nearly constant value for Lu over this same temperature range.

A comparison of the inset of Fig. 4 with Fig. 8, indicates that the maximum stiffening of the lattice (i.e., the peak in the Θ_D versus T plot) occurs at approximately the same temperature as the recovery peak of the quenched alloys, which is about the same as the anomaly temperature of the relaxed samples, again indicating the same origin of the various manifestations.

The various thermodynamic functions were calculated from the heat-capacity data. The standard room-temperature (298.15 K) values are

$$C_p = 26.44 \text{ J/g-at. K ,}$$

$$S_T^\circ = 47.04 \text{ J/g-at. K ,}$$

$$(H_T^\circ - H_0^\circ)/T = 20.04 \text{ J/g-at. K ,}$$

$$-(F_T^\circ - H_0^\circ)/T = 27.00 \text{ J/g-at. K .}$$

The complete set of thermodynamic functions from 2.5 to 300 K at 2.5 K intervals may be obtained by writing any of the authors.

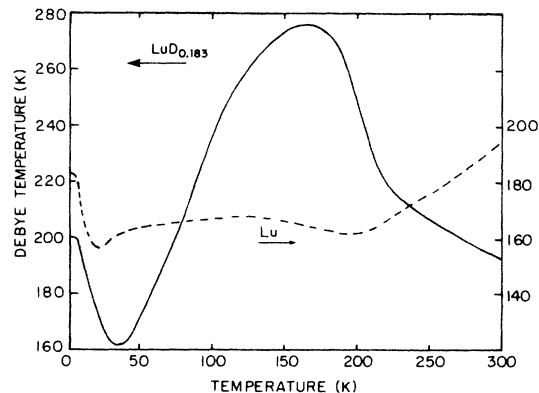


FIG. 8. Debye temperatures of Lu (dashed curve) and $\text{LuD}_{0.183}$ (solid curve) as a function of temperature. Note the difference in scales for the two materials—in actuality the Debye temperature of pure Lu is always less than that of $\text{LuD}_{0.183}$ except at room temperature where they are nearly equal.

ACKNOWLEDGMENTS

The help of L. Dumoulin in the electrical resistivity measurements is appreciated. Hydrogène et Défauts dans les Métaux is Unité No. 803 associée au Centre National de La Recherche Scientifique. The Ames Laboratory is operated for the U.S. Department of Energy by Iowa State University under Contract No. W-7405-ENG-82. Part of this work was supported by the Office of Basic Energy Sciences, U.S. Department of Energy.

*Permanent address: The Research Institute for Iron, Steel and Other Metals, Tohoku University, 2-1-1 Katahira, Sendai 980, Japan.

¹J. N. Daou, A. Lucasson, and P. Lucasson, *Solid State Commun.* **19**, 895 (1976).

²J. N. Daou, P. Vajda, M. Biget, A. Lucasson, and P. Lucasson, *Phys. Status Solidi A* **40**, 101 (1977).

³J. N. Daou, P. Vajda, A. Lucasson, P. Lucasson, and J. P. Burger, *Philos. Mag A* **53**, 611 (1986).

⁴P. Vajda, J. N. Daou, and P. Moser, *J. Phys. (Paris)* **44**, 543 (1983).

⁵R. Danielou, J. N. Daou, E. Ligeon, and P. Vajda, *Phys. Status Solidi A* **67**, 453 (1981).

⁶T. H. Metzger, P. Vajda, and J. N. Daou, *Z. Phys. Chem. N.F.* **143**, 129 (1985).

⁷J. N. Daou and P. Vajda, *J. Phys. F* **12**, L13 (1982).

⁸O. Blaschko, G. Krexner, J. N. Daou, and P. Vajda, *Phys. Rev. Lett.* **55**, 2876 (1985).

⁹B. J. Beaudry and K. A. Gschneidner, Jr., in *Handbook on the Physics and Chemistry of Rare Earths*, edited by K. A.

Gschneidner, Jr. and L. Eyring (North-Holland, Amsterdam, 1978), Vol. 1, p. 173.

¹⁰T.-W. E. Tsang, K. A. Gschneidner, Jr., F. A. Schmidt, and D. K. Thome, *Phys. Rev. B* **31**, 235 (1985).

¹¹T. Ito, B. J. Beaudry, K. A. Gschneidner, Jr., and T. Takeshita, *Phys. Rev. B* **27**, 2830 (1983).

¹²D. W. Boys and S. Legvold, *Phys. Rev.* **174**, 377 (1968).

¹³A. C. Damask and G. J. Dienes, *Point Defects in Metals* (Gordon and Breach, New York, 1963), p. 153.

¹⁴S. Legvold, *Phys. Rev. B* **3**, 1640 (1971).

¹⁵D. K. Thome, K. A. Gschneidner, Jr., G. S. Mowry, and J. F. Smith, *Solid State Commun.* **25**, 297 (1978).

¹⁶C. Kittel, *Introduction to Solid State Physics*, 4th ed. (Wiley, New York, 1971), p. 215.

¹⁷J. E. Kilpatrick and R. H. Sherman, Los Alamos National Laboratory Report No. LA-3114 (National Technical Information Service, U.S. Department of Commerce, Springfield, Virginia 22161) (unpublished).

¹⁸L. D. Jennings, R. E. Miller, and F. H. Spedding, *J. Chem. Phys.* **33**, 1849 (1960).